Urban Land-Cover Change Analysis in Central Puget Sound

Marina Alberti, Robin Weeks, and Stefan Coe

Abstract

A methodology was developed to interpret and assess land cover change between 1991 and 1999 in Central Puget Sound, Washington at several scales (landscape, sub-basins, and 90 m grid window) relevant to regional and local decision makers. Land cover data are derived from USGS Landsat (Thematic Mapper and Enhanced Thematic Mapper +) images of Central Puget Sound. Landsat data were registered, intercalibrated, and corrected for atmosphere and topography to ensure accuracy of land cover change assessment. We apply a hybrid classification method to each image to address the spectral heterogeneity of urbanizing regions. The method combines a supervised classification approach with a spectral unmixing approach to produce seven classes: >75 percent impervious, 15 to 75 percent impervious, forest, grass, clear cut, bare soil, and water. Land cover change is identified using the direct spatial comparison of classified images derived independently for each time period. We assess that the overall accuracy of each classified image was 91 percent for 1991 and 88 percent for 1999 respectively, which produces an accuracy of 85 percent for the change analysis. Our results show that urban growth over the last decade has produced an overall 6.7 percent increase in paved area.

Introduction

Remote sensing is a powerful tool for monitoring rapid changes in the landscape resulting from urban development. Landsat Thematic Mapper (TM) and Enhanced Thematic Mapper (ETM+) images provide moderate-resolution data sets over large geographic regions. These data are critical to both the natural and social sciences for quantifying urban landscape patterns and testing formal hypotheses about the relationships between urban patterns and various biophysical and ecological processes. Interpretation and analysis of urban landscapes from remote sensing, however, present unique challenges due to the spatial-temporal characteristics of urban land cover change which amplify the spectral heterogeneity of urban surfaces and make it extremely difficult to identify the source of observed change in observed reflectance.

The spectral heterogeneity of urban surface areas together with the spatial scale of urban phenomena cause significant subpixel mixing (Foody, 2000; Small, 2002). This is due to the complex mixtures of urban surface materials (i.e., concrete, wood, tiles, asphalt, metal, sand, and stone) and vegetation (grass, scrubs, shrubs, trees, and leaves) within the Landsat pixel resolution. Small (2002) indicates that while urban land cover classes can be distinguished when they occur in homogeneous regions larger than the spatial resolution of the sensor, this is rarely the case for moderate-resolution such as Landsat. The greatest challenge for urban land cover classification is to accurately determine the relative contribution of various materials that make up urban surface reflectance. An additional challenge is to compensate for temporal variability and changes in surface reflectance (such as seasonal variations) that are unrelated to land cover change (Hornstra, *et al.*, 1999; Small, 2002).

Previous studies have proposed various strategies to improve classification of urban landscapes. Ancillary data such as population, zoning, housing density and other information are frequently used in pre- and post-classification procedures (Harris and Ventura, 1995; Mesev, 1998; Vogelmann, *et al.*, 1998; Stuckens, *et al.*, 2000). Since urban areas typically have significant texture resulting from buildings and roads, analysts also use texture analysis in addition to spectral features to characterize urban land cover types (Gong and Howarth, 1990; Berberoglu, *et al.*, 2000; Stuckens, *et al.*, 2000; Stefanov, *et al.*, 2001). More recently, analysts have used data mining techniques, in particular artificial neural networks (Schalkoff, 1992; Paola and Schowengerdt, 1995; Berberoglu, *et al.*, 2000; Foody, 2001), to detect complex spectral urban patterns. Other analysts have emphasized classification strategies using multitemporal images (Martin and Howarth, 1989).

An alternative method for detecting urban land cover materials is spectral unmixing (Small, *et al.*, 2002). The Spectral Mixture Analysis (SMA) methodology (Adams, *et al.*, 1986) assumes that radiance from a heterogeneous surface mixes linearly within the Instantaneous Field of View (IFOV) according to the aerial percentages of each pure material present. According to this methodology, if a limited number of distinct endmembers are known *apriori*, it is possible to define a *mixing space* within which mixed pixels can be unmixed into percentages of constituent materials using a system of linear equations (Adams, *et al.*, 1986). A spectral unmixing approach is desirable in areas where features on the landscape are smaller than the spatial resolution of the satellite instrument (Small, 2002). This is especially true in urban areas where pixels are highly mixed. While spectral unmixing cannot reliably identify exact urban materials, it can determine relative amounts of vegetation and urban surfaces providing a good estimate for urban intensity.

In this study we integrate multiple pre-processing, land cover classification, and change analysis techniques to develop a methodology to interpret and assess land cover change between 1991 and 1999 in Central Puget Sound at

Marina Alberti is with the Department of Urban Design and Planning, University of Washington, Box 355740, Seattle, WA 98105 (malberti@u.washington.edu).

Robin Weeks is with the Department of Geological Sciences, University of Washington, Seattle, WA 98105.

Stefan Coe is with the Urban Ecology Research Laboratory, University of Washington, Seattle, WA 98105.

Photogrammetric Engineering & Remote Sensing
Vol. 70, No. 9, September 2004, pp. 1043–1052.

0099-1112/04/7009–1043/$3.00/0

Figure 1. Location Map for the Puget Sound Central Region. (Figure 1 is also available on the ASPRS Web site: www.asprs.org)

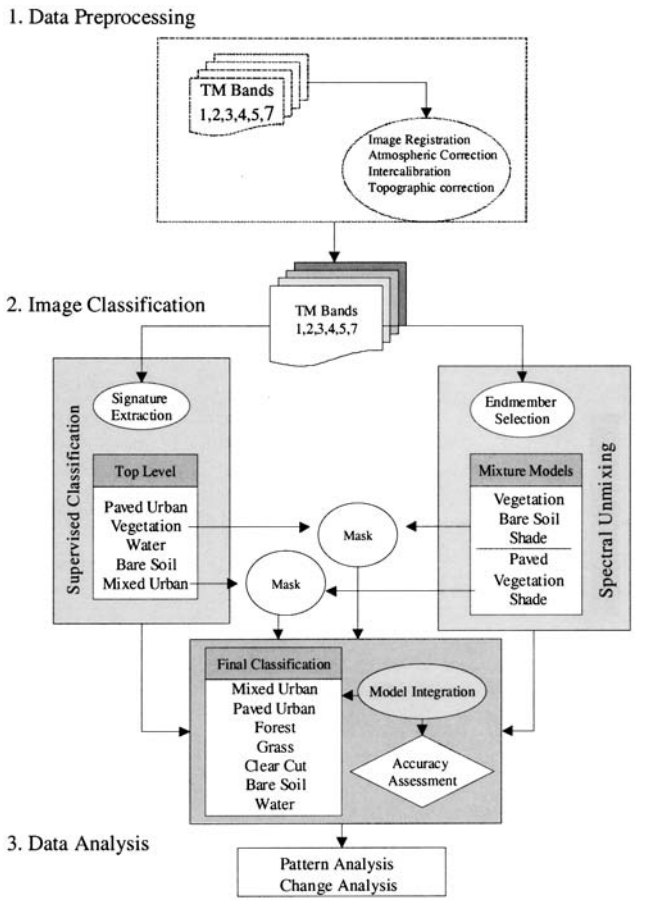

Figure 2. Image Processing and classification methodology.

several scales relevant to regional and local decision makers (Figure 1). We classify land cover using Landsat TM and ETM+ images of the Central Puget Sound, Washington from 1991 and 1999. We then perform a land cover change analysis between the two images at the landscape, regional, sub-basin, and 90 m grid scale.

The study focuses on the Central Puget Sound Region, which extends across four counties (King, Snohomish, Pierce, and Kitsap) with a total population of 3.3 million in 2000 (PSRC, 2001). The Central Puget Sound Region is one of the most rapidly growing and urbanizing regions in the United States. The total population and incorporated land have increased respectively by 19.2 percent and 48 percent since 1990 (PSRC, 2001). The study focuses particularly on lowland urban, suburban, and rural basins, which are increasingly affected by land cover change associated with urbanization. The remaining contiguous forests are quickly being replaced with fragmented urban landscapes. Growth is being moderately well regulated along a statute-defined urban-rural boundary, but the effectiveness of growth management strategies has not been established.

Image Processing and Classification

The methodology used in this project is summarized in Figure 2. Several image preprocessing steps were applied to make the images comparable before classification. We combine a supervised classification approach with a spectral unmixing approach (Adams, *et al.*, 1986; Gillespie, *et al.*, 1990; Smith, *et al.*, 1990) to discriminate among urban land cover classes. A supervised classification approach (using training sample areas and maximum likelihood distance thresholding) was used to discriminate across top-level classes. We then applied Spectral Mixture Analysis (SMA) methodology to *unmix* mixed pixels using a linear combination of the spectra of known endmembers. The challenge of SMA in urban landscapes is to accurately determine the relative contribution of different endmembers which make up the mixed pixel. For temporal analyses of images, the additional challenge is compensating for the temporal variation due to atmospheric or climatic factors.

Data Processing

Landsat satellite images from 1991, 1999, and 2000 were obtained for the Central Puget Sound Region to perform a land cover change analysis (Table 1). These images were all taken in July during peak foliage. The latter two are Landsat 7 and the former Landsat 5. All six VIS-SWIR light spectral bands were used in the study.

Image Rectification and Registration

The Landsat TM data were geocorrected to a UTM projection (Zone 10N, Spheroid Clarke 1866, Datum: NAD27). The 1991 image has been registered to a 30 m resolution Digital Elevation Model (DEM). Registration to a DEM is important for two primary reasons. First, the image is registered to real-world topographic features such as rivers, coastlines, ridges, and slopes. Most digital geographic data are associated with a digital elevation model, which enables the classified image to be compatible with other digital geographic data. Second, and most important, is that image registration to a DEM is required before a topographic (illumination geometry) correction can be applied to the image.

The 1991 image was registered to a Digital Elevation Model using a 1st-Order polynomial equation incorporating the location of known ground control points. The image was

TABLE 1. GENERAL INFORMATION FOR 1991 TM AND 1999 ETM+ IMAGES

	Data Characteristics			
Time	Sun Elevation (°)	Azimuth (°)	Resolution (meters)	RMS Error (control points)
7 July 1991	56	128	30	Reference
5 July 1999	60.35	138.37	30	.4(40)

resampled to 30 m resolution using nearest-neighbor resampling. The same methodology has been used to co-register the 1999 and 2000 images to the 1991 image. Points with high Root Mean Square Error (RMSE) were removed leaving about 50 points with an acceptable RMSE of 0.40 pixels. Registration of the 1999 and 2000 resulted in average RMSE less than one-half a pixel, and all images were resampled to 30 m pixel resolution.

Atmospheric Correction

Different surface types tend to have different spectral reflectance properties at specific wavelengths, and it is this property that allows features on the landscape to be distinguished in a multispectral image. However, there are other factors that can change the apparent spectral reflectance observed by a satellite which include the sensor calibration and atmospheric effects. Not only is a given object's spectral signature different at ground level than at the satellite sensor, it is also likely to vary temporally from image to image because of atmospheric changes with time (Miller, *et al.*, 1998). An additional source of change, not related to land cover change, is the seasonal variation in vegetation greenness.

A two-step approach is used to normalize the Landsat data. First, an atmospheric correction is applied to the 2000 image, which is considered the reference image. The 2000 image was chosen as the reference image because, as a Landsat 7 level 1G product, it has received superior radiometric correction compared to the 1991 Landsat 5 image. After this image has received the appropriate corrections, the 1991 and 1999 images are then inter-calibrated to the reference image.

The atmospheric correction model used for this project corrects for two main sources of error: atmospheric scattering and absorption. Atmospheric conditions affects radiance recorded by the sensor in two primary ways. First, some degree of incoming radiation, prior to reaching the earth's surface, is reflected and scattered by the atmosphere. Some of this *path radiance* is detected by the sensor and thus contributes a certain degree of noise that does not represent ground reflectance. Second, reflected energy from the earth's surface is absorbed by the atmosphere. The amount of energy that is transmitted through the atmosphere and recorded by the sensor depends on both wavelength and atmospheric constituents (Lillesand and Keifer, 1994). The first atmospheric affect can be corrected for by performing a dark object subtraction. Dark objects within the images, such as the ocean, are assumed to reflect close to zero radiation at all wavelengths in the VIS-SWIR. The amount of radiation that the satellite records for these objects can then be considered to be the amount of radiation that is scattered by the atmosphere, prior to reaching the ground. Subtracting a value representing dark objects from each band corrects for this particular effect. Before making any corrections, each band was converted from digital number to absolute units of radiance using the instrument derived calibration gains and offsets provided with the ETM+ image. Histograms for each band were visually inspected to determine a value representing the beginning of the histogram to the right of zero. These values were then subtracted from each band.

Determining average transmissivity values for each band and then dividing each band by its respective transmissivity value, corrects for error associated with absorption as radiation is reflected from the earth's surface and moves out through the atmosphere. We calculated transmissivity (Table 2) using MODTRAN© (http://www.vs.afrl.af.mil/Division/VSBYB/modtran4.html, last accessed 17 June 2004), a radiative transfer model that calculates the spectrally variant atmospheric transmissivity (τ), path radiance (Lp), and downwelling irradiance for a specific atmosphere (Berk, *et al.*, 1989). Transmissivity is simply the percentage of light at a given wavelength that is absorbed by the atmosphere. To restore the missing data that has been absorbed by the atmosphere, an appropriate atmospheric transmissivity must be calculated for each spectral band of the satellite sensor. This is done by convolving each band's spectral response function with the atmospheric transmissivity as a function of wavelength (calculated for a standard mid-latitude atmosphere). This is in effect a weighted average transmissivity value for each band's range of wavelength. Next, each band is divided by this value to complete the correction. This in effect, restores reflected energy that has been attenuated by the atmosphere (Miller, *et al.*, 1998).

TABLE 2. TRANSMISSIVITY VALUES FOR 2000 ETM+ IMAGE

	Radiometric Corrections		
	Gain	Bias/Offset	Transmissivity
Band 1	0.775686	−6.1999969	0.577586392
Band 2	0.795686	−6.3999994	0.639359791
Band 3	0.619216	−5	0.707731317
Band 4	0.96549	−5.1000061	0.787354206
Band 5	0.125726	−0.999981	0.896109355
Band 7	0.043726	−0.3500004	0.871986658

Inter-calibration

The atmospheric correction is applied only to the 2000 image. Since this image is a Landsat 7 ETM+ product we assume that the predominant source of data error is from the atmosphere and not instrument calibration. To correct the 1991 and 1999 image for atmosphere, they are simply inter-calibrated to the 2000 using the following process: pixel values from various materials that are assumed to have remained (relatively) unchanged through out the study period are taken from each image to use as inputs in a linear regression model for each of the six bands. To inter-calibrate the 1991 image, the gains and offsets from the regression equations are applied to each band. The result is that an invariant material will have the same spectral properties in the 1991 image as it has in the 2000 image. There are two main assumptions made for the inter-calibration procedure: one is that the effect of atmosphere is linear throughout the image, and the other is that we have identified unchanged pixels in the images.

It is important to note that the inter-calibration process does not eliminate the effects of seasonal changes that affect conditions on the ground. Climatic data show, for example, lower than average precipitation in 1991 and record high precipitation in 1999 (NOAA, 2001). The vegetation cover responds accordingly to these rainfall changes and is clearly greener in 1999. These effects need to be taken into account in the interpretation of land cover change analysis.

Topographic Correction

The orientation of the land surface with respect to the sun controls the amount of incident radiation, which in turn affects the amount of reflected radiation. Sun-facing slopes are brighter than shaded slopes. An image can be normalized for the effects of topography using several different techniques; we use a Lambertian topographic correction. This involves dividing each band of each image by a shaded relief model (the cosine of the solar incidence angle). First, a shaded relief model is calculated using a Digital Elevation Model and the sun's elevation angle and azimuth at the time and date of image acquisition. The result is a topographic image with a range from 0 to 1, with a value of 1 indicating a perfectly flat surface that is perpendicular to the incident solar radiation. As the range approaches zero, the greater is the impact of slope and solar position. Each atmospherically-corrected band is divided by the shaded relief model to normalize for

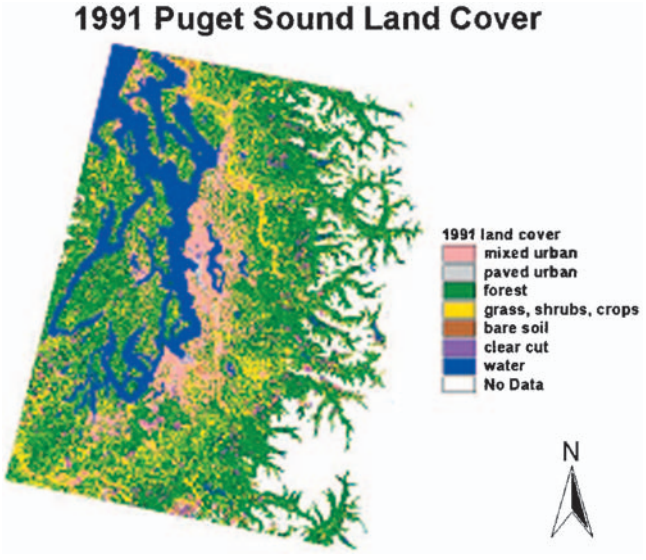

(a)

Plate 1a. Land Cover Classification 1991.

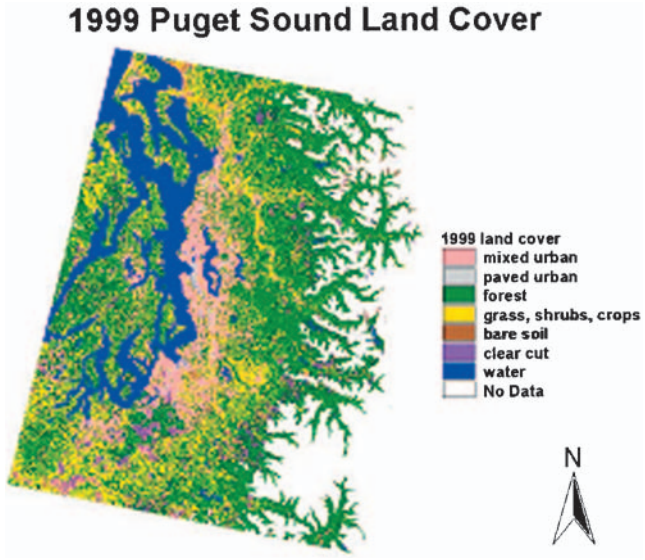

(b)

Plate 1b. Land Cover Classification 1999.

topography. Since this technique works only for gentle to moderate topography, each image has been subsetted to include only areas below 500 m.

Land Cover Classification

We develop a hybrid classification method to address the spectral heterogeneity characteristic of urbanizing landscapes. The classification methodology includes two steps that combine a supervised classification approach with a spectral unmixing approach based on fractions of endmembers. Spectral Mixture Analysis (SMA) assumes that a pixel's radiance is a linear combination of the radiance emitted by a limited number of spectral end-members (Adams, *et al.*, 1986; Gillespie, *et al.*, 1990; Smith, *et al.*, 1990). We first identify mixed urban pixels using a supervised classification that distinguishes between paved urban (>75 percent paved) and mixed urban pixels (<75 percent paved). We then apply a three end-member mixing model from which the percentage of impervious surface is derived. Spectral end-members (i.e., *pure* spectral classes) were developed by visual interpretation of the spectral feature space images and a supervised training sample set of known classes. The mixture model was used to estimate the relative proportions of the spectral end-members which were then used to classify into appropriate land cover types. Our final classification includes seven classes (Plate 1a and 1b, Tables 3 and 4).

Top Level Supervised Classification

Supervised classification includes three stages: training, allocation, and testing (Anderson, *et al.*, 1976; ERDAS©, 1997). Training is the identification of a sample of pixels of known class membership obtained from reference data. These training pixels are used to derive spectral signatures for classification, and signature statistics are evaluated to ensure adequate separability. Then, the pixels of the image are allocated to the class with greatest similarity to the training data metrics. An accuracy assessment is employed to assess the agreement of a random selected testing sample with ground truth points.

We applied a supervised top-level classification by extracting spectral signatures from homogenous surface types from the image using orthophotos as references. We define training samples and extract spectral signatures from these homogeneous areas. These signatures include water, pavement, coniferous forest, deciduous forest, grass, crops, shrub, and bare soil. These spectral signatures were combined to produce five categories that were applied to each image using a supervised classification: water, paved, mixed urban, vegetation (vegetation

TABLE 3. LAND COVER CLASSES UTILIZED IN VARIOUS CLASSIFICATION LEVELS

Top Level Classes	2nd Level Classification	Final Classification
Paved Urban	Paved Urban >75%	Paved Urban >75%
Mixed Urban	Mixed Urban >75%	
	Mixed Urban 15–75%	Mixed Urban 15–75%
	Mixed Urban <15%	(reassigned to vegetation)
Vegetation	Coniferous Forest	Forest
	Deciduous Forest	
	Grass Shrub Crops	Grass Shrub Crops
Bare Soil		Bare Soil
Clear Cut		Clear Cut
Water		Water

TABLE 4. LAND COVER CLASS DESCRIPTIONS FOR DETERMINING ASSIGNMENT IN CLASSIFICATION MODELS

Land Cover Class Description		
No.	Class	Definition
1	Mixed Urban	A combination of urban materials and vegetation. Predominantly low and mid-density residential
2	Paved Urban	Surfaces with an impermeable area >75%. This includes high-density development, parking lots, streets and roof tops
3	Forest	Surface dominated by trees
4	Grass, Shrubs, Crops	Agricultural fields, golf courses, lawns and regrowth after clear cuts
5	Bare Soil	Land that has been cleared, rocks and sand
6	Clear Cut	Clear cut forest that has not had significant regrowth and very dry grass
7	Water	Lakes, reserviors, streams

classes combined), and bare soil. These classes are then used as a mask for the second-level classification. Bare soil, pavement, and water are considered to be classified at this top-level stage, meaning they will not undergo any further classification. Spectral unmixing is then applied to the mixed urban and vegetation classes only.

Spectral Unmixing Applied to Mixed Urban

A spectral unmixing model based upon pixel constituents in the mixed urban class is applied to the *mixed urban* image. The end-members have been determined to be pavement, green vegetation, and shade. The results of the unmixing analysis are three end-member fraction images and an error image. Error terms (expressed as RMSE) indicate the average error for each pixel across all bands (Rashed, *et al.*, 2001). The RMSE is used to assess the results of the model. If the fractions are normalized to exclude the shade fraction, then the fraction image contains a percentage value for each cell indicating the aerial proportion of that end-member in the pixel in question. The aerial percentages are thus calculated for vegetation and pavement only. Finally, the fraction images are reclassified into ranges.

Specifications of finer classification of urban land cover depend on the uses that the data will need to serve. The primary motivation for this analysis is determining changes in categories representing different degrees of impervious surface. Using the spectral unmixing output we reclassify urban classes to greater than 75 percent paved and between 15 to 75 percent paved for minimizing error in the change analysis. Using a 3×3 nearest neighbor focal majority filter, we reassigned pixels below 15 percent impervious surface to the dominant class in the neighborhood.

Spectral Un-mixing Applied to Vegetation

We apply a spectral un-mixing model using green vegetation, shade, and bare soil end-members to the vegetation class to identify grass and forest classes. We use the shade endmember fraction image to differentiate between grass and forest cover. The shade endmember fraction image was used to discriminate between grass (including grass, shrub, and crops), deciduous forest, and coniferous forest. This was achieved by examining the shade fraction histogram for image subsets of known vegetation type. Shade cutoff values for each vegetation type were determined based upon the histograms for each vegetation type. The final breakdown is as follows: Grass: $\leq$32 percent shade, Deciduous: $>$32 percent and $<$52 percent shade, and Conifer: $\geq$52 percent shade. Unfortunately, The conifer and deciduous classes were not separable at a sufficient accuracy level according to a preliminary accuracy assessment and were combined into a combined forest class.

Bare Soil and Clear Cuts

Agricultural bare soils and clear cuts proved difficult to separate from pavement and mixed urban classes, since their spectral signatures are similar. Clear cuts are composed of slash, vegetation, and soil which is spectrally similar to the mixed urban class that is a mix of vegetation and pavement. The result was that some urban pixels were classified as clear cut or agricultural bare soil and vise versa. For the most part, the misclassified pixels were relatively isolated producing a *salt and pepper* look. We apply the following techniques to isolate and remove the clear cut and agricultural bare soil pixels from the image. Using the assumption that forest clearcuts should comprise at least several contiguous pixels, first a 5×5 nearest-neighbor filter was applied to the top-level supervised classification. This resulted in a smoothed image that eliminated isolated pixels and produced clumps of contiguous land cover types. Then, binary mask images were created for both bare soil and clear-cut pixels. The *clump* operation in ERDAS© was applied to each binary image to clump pixels with their connecting neighbors to form discrete patches. We used the *sieve* operation in ERDAS© to keep only those patches of clear-cut and bare soil that were greater than 40 pixels in area. This enabled us to eliminate small patches of clear-cut and bare soil that might have been misclassified as pavement, mixed urban or dry grass. We assume that clear cuts and agricultural bare soil are larger than 40 pixels in area and that isolated pixels that were classified as clear cut and bare soil are most likely not either of those classes.

The *sieve* operation results in final classes for both clear-cut and agricultural bare soil. A masking approach is then used to remove these pixels from the actual image. A second top-level supervised classification is applied to the image without the agricultural bare soil and clear-cut pixels. This includes signatures for water, paved urban, mixed urban, vegetation, and a barren land use class (representing non-agricultural bare soil). The barren land class behaved similarly to agricultural bare soil, resulting in many isolated pixels that should have been classified as paved. Another 5×5 filter was applied only to the barren land class to reassign isolated pixels. The barren land class is then merged with the agricultural bare soil class to make one bare soil class. Paved urban and water are considered classified and removed from the image. Vegetation pixels and mixed urban pixels are separated into two distinct images.

Final Classified Image

The final classified image consists of paved urban ($>$75 percent paved), mixed urban (between 15–75 percent paved), grass (grass, shrub, and crops), forest (conifer and deciduous), clear cut, bare soil, and water. The paved urban class includes the top level classification paved and the part of the mixed urban class $>$75 percent impervious extracted from spectral unmixing. The mixed urban class is split into three categories: below 15 percent impervious, between 15 to 75 percent impervious and greater than 75 percent impervious. Pixels below 15 percent impervious are reassigned to their neighboring classes via a 3×3 nearest neighbor focal majority filter. Pixels between 15 to 75 percent impervious constitute a distinct mixed urban class. Deciduous and coniferous forest are combined into a combined forest class.

Accuracy Assessment

The accuracy was determined by comparing known *control* points in digital orthophotos to the equivalent sites in the classified scene (Foody, 2002). We generate an error matrix, a user's and producer's accuracy assessment, and a Kappa coefficient for each classification. Kappa Statistic is an index that compares the agreement against what might be expected by chance. Kappa is the chance-corrected proportional agreement, and its possible values range from +1 (complete agreement) through 0 (no agreement above that expected by chance) to −1 (complete disagreement). Error matrices for both images are in Tables 5 and 6.

We randomly selected approximately 400 points for each image to perform the accuracy assessment (approximately 50 points for each class) using ERDAS©. We defined a 3×3 pixels window size for the assessment. The center pixel assignment is determined based on a cluster of uniformly classified pixels within the window. Coordinates from the center pixel are used to create a vector grid showing each 3×3 window centered on the center pixel. This coverage is used as an overlay reference when comparing the classes to the digital orthophotos. The windows are overlaid on the orthophotos so that 3×3 spatial dimensions of the 3×3 pixels are clearly defined when performing the assessment.

A top-level classification accuracy assessment is applied to the 1999 image to make sure the top-level classification is

TABLE 5. ACCURACY ASSESSMENT FOR 1991 LAND COVER CLASSIFICATION

Accuracy Assessment 1991										
		Observed								
		Mixed Urban (15–75% Impervious)	Paved (>75% Impervious)	Forest	Grass	Bare Soil	Clear Cut	Water	Totals	User's Accuracy
Classified	Mixed urban (15–75% Impervious)	46	4	0	0	0	0	0	50	92.0%
	Paved (>75% Impervious)	1	47	0	0	0	0	0	48	97.9%
	Forest	0	0	45	0	0	3	0	48	93.8%
	Grass	0	0	2	38	0	10	0	50	76.0%
	Bare Soil	0	0	1	0	41	0	0	42	97.6%
	Clear Cut	0	0	2	3	0	43	0	48	89.6%
	Water	0	0	0	0	0	0	50	50	100.0%
	Totals	47	51	50	41	41	56	50	336	
	Producer's Accuracy	97.9%	92.2%	90.0%	92.7%	100.0%	76.8%	100.0%		
						Observed Agreement		0.923		
						Kappa Coefficient		0.910		

TABLE 6. ACCURACY ASSESSMENT FOR 1999 LAND COVER CLASSIFICATION

Accuracy Assessment 1999										
		Observed								
		Mixed Urban (15–75% Impervious)	Paved (>75% Impervious)	Forest	Grass	Bare Soil	Clear Cut	Water	Totals	User's Accuracy
Classified	Mixed Urban (15–75% Impervious)	43	1	1	4	1	0	0	50	86.0%
	Paved (>75% Impervious)	1	46	0	0	3	0	0	50	92.0%
	Forest	0	0	70	1	0	0	0	71	98.6%
	Grass	1	0	0	48	0	0	0	49	98.0%
	Bare Soil	0	2	1	1	46	0	0	50	92.0%
	Clear Cut	0	0	0	18	3	28	0	49	57.1%
	Water	0	0	0	0	0	0	50	50	100.0%
	Totals	45	49	72	72	53	28	50	369	
	Producer's Accuracy	95.6%	93.9%	97.2%	66.7%	86.8%	100.0%	100.0%		
						Observed Agreement		0.897		
						Kappa Coefficient		0.879		

accurate enough to warrant sub-pixel classification for the mixed urban classes. Since the results from the top-level classification accuracy assessment supported the classification methodology, we completed the accuracy assessment of top and sub-pixel classification classes for 1991 and 1999. Randomly selected pixels for each class are compared to the digital orthophotos using the following decision rules to produce a confusion matrix:

- Paved Urban: A clear majority of the pixel in the window is paved (impervious surface >75 percent), i.e. streets, rooftops, parking lots. We know that coastlines and edges of rivers and lakes often get classified as paved. These will not be counted as wrong, but they will be masked out.
- Mixed Urban: The window contains vegetation and evidence of development (impervious surface is between 15 and 75 percent), i.e. parts of houses, roads, garages.
- Water: A clear majority (>75 percent) of the window is water.
- Bare Soil: A clear majority (>75 percent) of the window is bare soil.
- Forest: A clear majority (>75 percent) of the window is forested.
- Grass/shrub/crops: A clear majority (>75 percent) of the area is grass, crops or shrub.
- Clear Cut/cleared land: This class has picked up on a few types of covers that are very related, including clear cuts, very dry grass, shrub and recently cleared land for development. If a majority of these cover types exist in the window, then it has been accurately classified.
- Mixed Urban unmixing: The results of the unmixing analysis are three end-member fraction images. We use these fractions to calculate the percentage of impervious and vegetation.

Results are converted to themes based on ranges of percentage of impervious. Ranges of Mixed Urban used for the classification include: >75 percent impervious, 15 percent–75 percent impervious and <15 percent impervious. We use the same methodology for sampling and accuracy assessment of the disaggregated urban categories. Ranges of impervious surface within categories are compared to actual amounts of

impervious surface and vegetation within each 3 × 3 pixel window. For the 1991 image, an accuracy assessment is performed on the final 1991 classified image (instead of treating top-level and unmixed categories separately).

Overall assessment indicates that the classification is highly accurate at the 90 m resolution. Kappa coefficients in 1991 and 1999 were respectively 0.92 and 0.88. Accuracy of individual classes vary. Paved urban, mixed urban, and forest are the most accurate classes, clear cuts and bare soil are the least accurate. The limiting factor in our accuracy assessment is the limited spatial extent of the digital orthophotos. This has reduced the number of sample points available to assess the accuracy of these last two categories.

Change Analysis

The change detection technique employed is based on a pixel by pixel comparison of land cover derived independently for each time period (Richards and Xiuping, 1999). The change analysis and smoothing procedure are illustrated in Figure 3.

Change Detection

Change detection involves comparing one date of imagery to a second date that has been registered and intercalibrated to the first. Several iterations of the change analysis provided important feedback that helped formulate our final methodology (Figure 2). The spatial resolution and actual classifications used in the change analysis has been adjusted to incorporate this new information. The various change analysis iterations indicated the extent to which errors associated with registration and spatial heterogeneity (complex local texture) affected the analysis. The effect of different climatic regimes in the two time periods and resulting impacts on maturing vegetation were observed to impact the accuracy of the change analysis for several classes. Most obvious were pixels that had gone from mixed urban in 1991 back to forest or grass in 1999. Such pixels were typically isolated and located in older, lower density residential neighborhoods comprised of mixed, heterogeneous surface types. Air photo comparisons from 1990 and 1999 confirmed that this error was due to a combination of the aforementioned seasonal climatic factors.

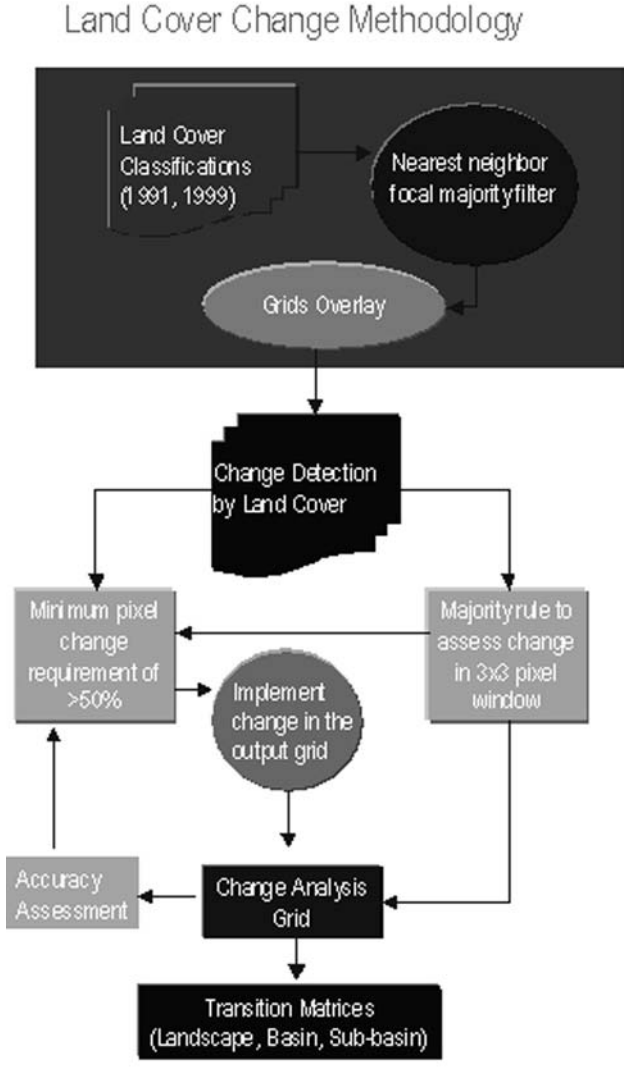

Figure 3. Land Cover Change Methodology.

The 1991 and 1999 classified images are converted to change codes prior to the overlay/change analysis process (Table 5). The two grids are then compared to create an output grid containing values indicating if a cell changed class and the nature of that change. The land cover grids were overlaid (added) resulting in one grid (referred to as the *change grid* hereafter) with unique values for each type of scenario (e.g., forest-forest = 44, forest-mixed urban = 42). Using a moving window analysis, additional grids were calculated for each change class (in the change grid) representing the number of immediate neighbors sharing the same value. For example, if a pixel has a value of 42, and 4 of its immediate neighbors also had a value of 42, the corresponding grid cell would return a value of 4. This computation was done for each class individually resulting in separate grids for each class.

A set of decision rules was then established to determine whether a grid cell had changed classes or remained the same. In order for a cell to switch from one type to another, a minimum number of cells in its immediate neighborhood also had to change to the same cover type. Problems associated with mis-registration and landscape heterogeneity make it difficult to measure change at the individual pixel level. Moreover, anthropogenic landscape changes (recognizable by Landsat 5 and 7) typically occur in areas larger than a 30 × 30 m grid cell. We have chosen this method over resampling to a courser resolution, which does not necessarily filter out error associated with mis-registration, mis-classification, or landscape heterogeneity. The following decision rules were used after various iterations of land cover change accuracy:

- Forest to Paved and Mixed Urban: at least five of the pixels in a 3 × 3 window have to change from forest to Mixed urban or Paved urban. Change to Paved Urban or Mixed Urban is determined by the majority rule.
- Changes from Mixed Urban to other land cover classes are implemented with a more conservative threshold: at least six of the pixels in a 3 × 3 window have to change from Mixed Urban to other land cover classes in order for the land cover change to be implemented. This higher threshold is justified by the higher heterogeneity of the Mixed Urban class.
- All other changes: at least five of the pixels in a 3 × 3 window have to change from the original class to the changed class.
- Pixels not fitting into any of these criteria were assigned to their 1991 classes.

Change Analysis Accuracy

We randomly select approximately 730 points on the change image to perform the accuracy assessment of the change analysis (approximately 40 points for each class change). The accuracy assessment methodology uses the same approach applied for the classification. Randomly selected pixels in each change class are compared to change observed by comparing digital orthophotos for 1991 and 1999. We assess both pixels that have changed and pixels that have remained the same.

We distinguish the accuracy of the change analysis by separating the error matrices of the individual classification from the error matrix of change detection. The latter is constructed from points that we have determined to be correctly classified. In this way we can discriminate between the accuracy of individual classes from the accuracy of individual class changes.

Overall accuracy is 0.85, but the accuracy of individual class changes vary considerably. It is particularly noticeable that our change analysis is conservative in the sense that change classes of pixels that have remained the same are highly accurate. Relatively high accuracy is observed for the classes that have changed from forest to mixed urban (90 percent) and to bare soil (88 percent) and lower accuracy for classes that have changed from grass or bare soil to mixed urban (65 percent). Less accurate but still within acceptable level of accuracy are the change classes from mixed urban to paved (80 percent) and bare soil to paved (83 percent).

Results

The magnitude of land cover change over the period 1991 to 1999 in Central Puget Sound is summarized in the change matrices (Tables 7, 8, and 9). We analyze land cover changes

TABLE 7. REGIONAL CHANGE ANALYSIS

Change Analysis: Entire Image below 500 m in hectares

		1999							
		Mixed Urban %	Paved %	Forest %	Grass %	Bare Soil %	Clear Cut %	Water %	Total Area (ha)
1991	Mixed Urban	93.8%	0.8%	0.7%	2.2%	0.6%	1.8%	0.1%	207426
	Paved	2.4%	85.8%	0.3%	2.5%	2.4%	1.1%	5.3%	42823
	Forest	1.9%	0.4%	85.4%	8.9%	0.3%	2.9%	0.3%	765137
	Grass	3.2%	0.6%	11.2%	80.9%	1.4%	2.5%	0.2%	311806
	Bare Soil	6.8%	3.6%	0.5%	5.9%	78.2%	0.7%	4.3%	23457
	Clear Cut	4.1%	0.7%	16.6%	43.6%	1.0%	33.7%	0.3%	36522
	Water	0.1%	0.3%	2.1%	0.1%	0.1%	0.0%	97.3%	311001
	Total Area (ha)	223646	45695	702332	343415	27905	46369	308808	1698171

TABLE 8. METROPOLITAN AREA CHANGE ANALYSIS

Change Analysis: Seattle-Bellevue-Everett PMSA in hectares

		1999							
		Mixed Urban %	Paved %	Forest %	Grass %	Bare Soil %	Clear Cut %	Water %	Total Area (ha)
1991	Mixed Urban	95.9%	0.7%	0.7%	1.9%	0.4%	0.3%	0.1%	110867
	Paved	2.6%	90.4%	0.3%	2.3%	1.9%	0.5%	2.0%	22485
	Forest	1.7%	0.2%	90.0%	5.8%	0.2%	2.1%	0.1%	316417
	Grass	3.5%	0.7%	12.2%	80.4%	1.8%	1.2%	0.1%	125085
	Bare Soil	7.9%	4.3%	0.7%	8.0%	75.7%	0.5%	2.9%	10264
	Clear Cut	3.8%	0.5%	36.5%	39.5%	1.0%	18.5%	0.0%	13911
	Water	0.2%	0.3%	17.0%	0.4%	0.5%	0.1%	81.5%	29859
	Total Area (ha)	117993	23250	310978	127969	11845	11290	25564	628889

TABLE 9. CHANGE MATRIX IN SEVEN WASHINGTON WATER RESOURCE INVENTORY AREAS

Land Cover Summary by Watershed

Watershed Resource Inventory Area	Year	Mixed Urban %	Paved %	Forest %	Grass %	Bare Soil %	Clear Cut %	Water %	Total Hectares
WRIA 7 Snohomish	1991	8.6%	1.7%	58.4%	20.3%	1.3%	2.9%	6.7%	244771
	1999	9.5%	1.8%	59.0%	19.8%	1.5%	2.4%	5.9%	
WRIA 8 Cedar-Sammamish	1991	31.7%	5.1%	32.6%	11.3%	1.4%	0.2%	17.7%	150729
	1999	33.2%	5.5%	31.4%	10.8%	1.5%	0.2%	17.4%	
WRIA 9 Duwamish-Green	1991	24.2%	6.9%	32.7%	19.9%	1.6%	1.8%	12.8%	94021
	1999	25.3%	7.3%	32.2%	19.3%	1.8%	1.7%	12.5%	
WRIA 10 Puyallup-White	1991	20.5%	4.4%	40.1%	24.5%	3.2%	2.1%	5.2%	97954
	1999	22.6%	4.9%	35.2%	26.0%	3.6%	2.7%	5.0%	
WRIA 11 Nisqually	1991	8.4%	1.3%	59.1%	25.1%	0.6%	2.9%	2.6%	114163
	1999	8.7%	1.4%	51.9%	27.4%	1.1%	6.8%	2.6%	
WRIA 12 Chambers-Clover	1991	37.3%	6.4%	28.9%	13.9%	1.7%	1.5%	10.3%	46428
	1999	40.5%	7.4%	23.8%	12.6%	2.3%	3.0%	10.4%	
WRIA 13 Deschutes	1991	14.8%	2.7%	45.9%	22.5%	1.2%	2.5%	10.4%	66999
	1999	16.6%	3.3%	38.1%	26.0%	1.7%	3.6%	10.8%	
WRIA 15 East Kitsap	1991	8.4%	1.4%	44.2%	12.0%	1.0%	0.9%	32.0%	255062
	1999	9.5%	1.6%	41.0%	13.0%	1.0%	1.6%	32.2%	

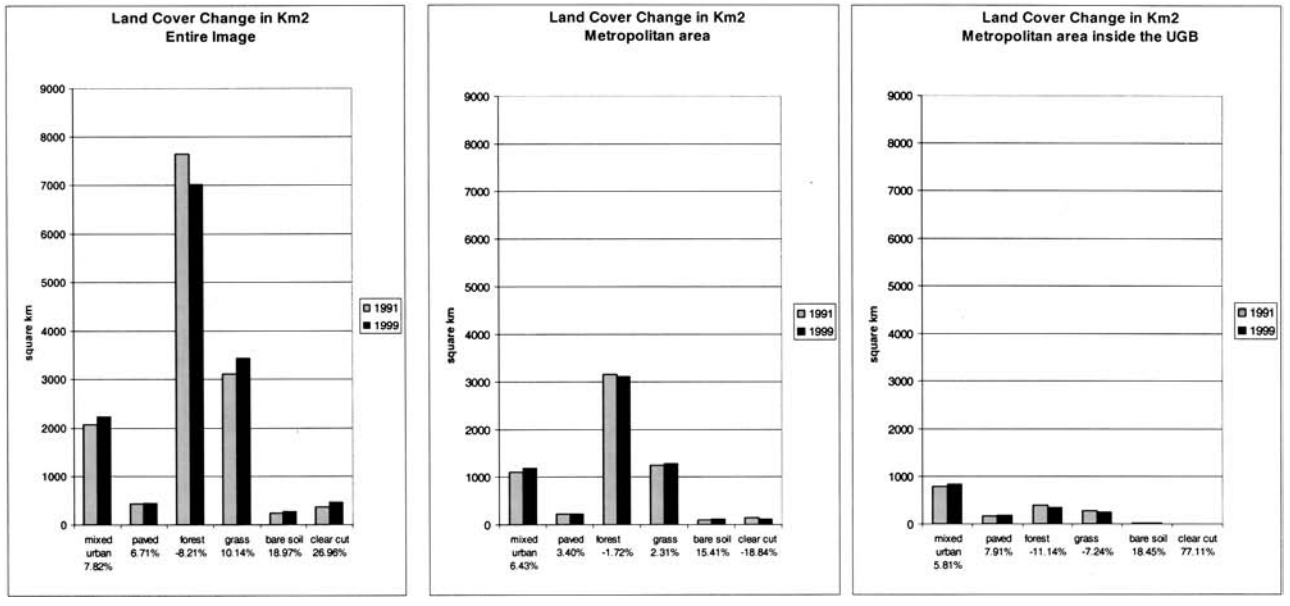

(a) (b) (c)

Figure 4. Land cover change for entire image (a), Seattle metropolitan area (b), and metropolitan area inside the urban growth boundaries (c).

within the Central Puget Sound region with elevations below 500 meters. We summarize the results for the entire image (Table 7, Figure 4a), the Seattle Metropolitan area (Table 8, Figures 4b and 4c), and nine Washington Water Resource Inventory Areas (WRIA) (Table 9).

Using the developed area including paved urban (>75 percent impervious) urban and mixed urban (between 25 percent and 75 percent impervious) in 1991 as a baseline, the area covered by development within the entire study area (the Central Puget Sound Region) increased respectively by 28 ± 4 km^2 and 162 ± 24 km^2, representing a 6.7 percent increase in paved urban and a 7.8 percent increase in mixed urban areas (Figure 4a). Overall the region has added 1 percent of the total area to development. Forest cover has declined by 628 ± 94 km^2 a 8.2 percent decline over the same period. Overall the region has lost forest cover corresponding to 5 percent of the total area.

Almost half of the land conversion to development has occurred in the Seattle metropolitan area with about 80 ± 12 km^2 land converted to mixed and paved urban, a 6 percent increase in overall developed area since 1991 (Figure 4b). The most intense development has occurred primarily within the urban growth boundary (UGB) where the increase in paved area accounts for 13 ± 1.9 km^2, a 7.9 percent increase (Figure 4c). The increase in mixed urban area adds to 45 ± 6.7 km^2, a 5.8 percent increase over the 1991 baseline. This represents a 2.6 percent increase in the total metropolitan area within the UGB being now mixed urban area and about 1 percent more of the total metropolitan area within the urban growth boundaries now paved. Forest areas have declined by about 44 ± 6.6 km^2 within the UGB boundaries an 11.1 percent decrease over the same period.

Conversion of forestland to mixed urban and paved is also marked in WRIA 8, 10, 11, 12, and 13. More than 2 percent of the Cedar-Sammamish watershed (WRIA 8) area has been converted to urban land. This represents more than 4.3 percent of 1991 forest land and 5.3 percent of 1991 grass land converted to mixed urban and paved urban over the eight-year period. Similar trends can be observed for Duwamish-Green (WRIA 9), Nisqually (WRIA 11) and Deschutes (WRIA 13). Even more marked are the changes in Puyallup-White (WRIA 10) and Chambers-Clover (WRIA 12) where the loss of forest land to clear cuts and development accounts respectively 7 percent and 5 percent of the total area.

Conclusions

The objective of this project was to discriminate categories of urban land cover using USGS Landsat TM and ETM+ images of the Puget Sound (Washington) from 1991 and 1999 and to perform a land cover change analysis between the two images. Specific objectives of the study are: (1) to develop a protocol to process and classify the land cover to explicitly discriminate a number of land cover classes that effectively represent a mix of impervious surfaces and natural vegetation; and (2) to perform a land cover change analysis at the regional and watershed scales.

We combine a supervised classification approach with a spectral unmixing approach to discriminate among seven urban land cover classes. Transition matrices were derived for the entire image, at the metropolitan scale, and at the basin level to enable comparisons and analysis in relation to socio-economic, ecological, and hydrological processes. Change images were also created to quantify and display the changes to land cover that occurred between two time periods for target land cover classes. The images capture key trends such as the loss of forested land to urban development or to grass, shrubs, and crops, reflecting re-growth after timber harvests.

Registration errors and seasonal variations necessitated a degradation in the spatial resolution of the change analysis from the 30 m pixel resolution; overall assessment indicates that the classification is highly accurate at a 90 m resolution. Kappa coefficients in 1991 and 1999 were respectively 92 percent and 88 percent. Individual class user's accuracy ranged from 76 percent (grass) to 98 percent (paved urban) for 1991 and from 57 percent (clear cut) to 99 percent (forest) for 1999. 100 percent of the water pixels were accurately classified in both years. The overall accuracy of the change analysis is 85 percent, with higher accuracy observed for the

classes that have changed from forest to mixed urban (90 percent) and to bare soil (88 percent) and lower accuracy for classes that have changed from grass or bare soil to mixed urban (65 percent). The methodology described here is currently being refined to improve separability of vegetation classes by using multiple images and leaf-off additional images of the same years.

Acknowledgments

Funding for this project was provided by the Washington State Puget Sound Water Quality Action Team and the National Science Foundation Biocomplexity Program (BCS 0120024). The authors would like to thank Derek Booth (UW Department of Civil and Environmental Engineering) and Kristina Hill (UW Department of Landscape Architecture) for their comments on an initial report on this project. We thank also Doug Myers (WA Puget Sound Water Quality Action Team) and Pete Dowty (WA Puget Sound Water Quality action Team) for their careful review of the data. We also thank Erik Stronberg for editorial assistance.

References

Adams, J.B., M.O. Smith, and P.E., Johnson, 1986. Spectral mixture modeling: A new analysis of rock and soil types at the Viking Lander 1 site, *Journal of Geophysical Research,* 91(B8):8098–8122.

Adams, J.B., M.O. Smith, D.E. Sabol, V. Kapos, R.A. Filho, D.A. Roberts, and A.R. Gillespie, 1995. Classification of multispectral images based on fractions of endmembers: Application to land cover change in the Brazilian Amazon, *Remote Sensing of Environment,* 52(2):137–154.

Anderson, J.R., *et al.*, 1976. A Land Use and Land Cover Classification System for use with remote sensor data, *U.S. Geological Survey Professional Paper* 964.

Berberoglu, S., C.D. Lloyd, P.M. Atkinson, and P.J. Curran, 2000. The integration of spectral and textural information using neural networks for land cover mapping in the Mediterranean, *Computers and Geosciences*, 26(4):385–396.

Berk, A., L.S. Bernstein, and D.C. Robertson, 1989. *MODTRAN: A Moderate Resolution Model for LOWTRAN 7*, GL-TR-89-0122, Spectral Sciences, Inc., Burlington, Massachusetts, p. 19.

ERDAS©, 1997. ERDAS Field Guide, Fourth Edition, ERDAS©, Inc; USA. 656 p.

Foody, M.G., 2001. Thematic mapping from remotely sensed data with neural networks: MLP, RBF and PNN based approaches, *Journal of Geographical Systems*, 3(3):217–232.

Foody, M.G., 2002. Status of land cover classification accuracy assessment, *Remote Sensing of Environment*, 80(1):185–201.

Gillespie, A.R., M.O. Smith, J.B. Adams, S.C. Willis, A.F. Fischer III, and D.E. Sabol, 1990. Interpretation of residual images: spectral mixture analysis of AVIRIS images, Owens Valley, California, *Proceedings of the 2nd Airborne Visible/Infrared Imaging Spectrometer (AVIRIS) Workshop*, Pasadena, California, 243–270. (Jet Propulsion Laboratory, JPL Publication 90–54)

Gong, P., and P.J. Howarth, 1990. The use of structural information for improving land-cover classification accuracies at the rural-urban fringe, *Photogrammetric Engineering & Remote Sensing*, 56(1): 67–73.

Harris, P.M., and S.J. Ventura, 1995. The integration of geographic data with remotely sensed imagery to improve classification in an urban area, *Photogrammetric Engineering & Remote Sensing*, 61(8):993–998.

Hornstra, T.J., M.J.P.M. Lemmens, and G.L.Wright, 1999. Incorporating intra-pixel reflectance variability in the multispectral classification process of high-resolution satellite imagery of urbanized areas, *Cartography*, 28(2):1–9.

Lillesand, T.M., and R.W. Keifer, 1994. *Remote Sensing and Image Interpretation*, 3rd edition, Wiley Publishers, New York, 750 p.

Martin, L.R.G., and P.J. Howarth, 1989. Change-Detection Accuracy Assessment Using SPOT Multispectral Imagery of the Rural-Urban Fringe, *Remote Sensing of Environment*, 30(1):55–66.

Miller, A.B., E.S Bryant, and R.W. Birnie, 1998. An analysis of land cover changes in the Northern Forest of New England using multitemporal Landsat MSS data, *International Journal of Remote Sensing*, 19(2):245–265.

Mesev, V., 1998. The use of census data in urban image classification. *Photogrammetric Engineering & Remote Sensing*, 64(5):431–438.

NOAA, 2001. Climatological Data. World Center for Meteorology: National Climatic Data Center, Asheville, North Carolina.

Paola J.D., and R.A. Schowengerdt, 1995. A detailed comparison of backpropagation neural network and maximum-likelihood classifiers for urban land use classification, *IEEE Transactions on Geoscience and Remote Sensing*, 33(4):981–996.

PSRC, 2001. Decennial Change in Population and Land Area of Cities, Towns, and Counties in the Central Puget Sound: 1990 to 2000. US Census 2000. P.L. 94-171 Redistricting Data. Puget Sound Regional Council.

Rashed, T., J. Weeks, M. Gadalla, and A. Hill, 2001. Revealing the Anatomy of Cities through Spectral Mixture Analysis of Multispectral Satellite Imagery: A Case Study of the Greater Cairo Region, Egypt, *Geocarto International*, 16(4):5–16.

Richards, J.A., and J. Xiuping, 1999. *Remote sensing digital image analysis*, Springer Publications, New York, 363 p.

Schalkoff, R.J., 1992. *Pattern recognition: statistical, structural and neural approaches*, John Wiley & Sons, USA, 1992.

Small, C., 2002. Multitemporal analysis of urban reflectance, *Remote Sensing of Environment*, 81(2-3):427–442.

Smith, M.O., S.L. Ustin, J.B. Adams, and A.R. Gillespie, 1990. Vegetation in deserts: I. A regional measure of abundance from multispectral images. *Remote Sensing of Environment*, 31(1):1–26.

Smith, M.O., S.L. Ustin, J.B. Adams, and A.R. Gillespie, 1990. Vegetation in deserts: II. Environmental influences on regional abundance, *Remote Sensing of Environment*, 31(1):1–26.

Stefanov, W.L., M.S. Ramsey, and P.R. Christensen, 2001. Monitoring urban land cover change: An expert system approach to land cover classification of semiarid to arid urban centers, *Remote Sensing of Environment*, 77(2):173–185.

Stuckens, J., P.R. Coppin, and M.E. Bauer, 2000. Integrating contextual information with per-pixel classification for improved land cover classification, *Remote Sensing of Environment*, 71(3):282–296.

Vogelmann, J.E., T. Sohl, and S.M. Howard, 1998. Regional characterization of land cover using multiple sources of data, *Photogrammetric Engineering & Remote Sensing*, 64(1):45–57.

(Received 10 December 2002; accepted 17 June 2003; revised 30 July 2003)